Continuously Improving Model of Road User Movement Patterns using Recurrent Neural Networks at Intersections with Connected Sensors

Julian Bock[1], Philipp Nolte[2] and Lutz Eckstein[1]
[1]Institute for Automotive Engineering (ika), RWTH Aachen University, Steinbachstr. 7, Aachen, Germany
[2]RWTH Aachen University, Aachen, Germany

Keywords: Prediction, Vulnerable Road Users, Pedestrian, Deep Learning, Automated Driving, Intersections.

Abstract: Intersections with connected infrastructure and vehicle sensors allow observing vulnerable road users (VRU) longer and with less occlusion than from a moving vehicle. Furthermore, the connected sensors are providing continuous measurements of VRUs at the intersection. Thus, we propose a data-driven prediction model, which benefits of the continuous, local measurements. While most approaches in literature use the most probable path to predict road users, it does not represent the uncertainty in prediction and multiple maneuver options. We propose the use of Recurrent Neural Networks fed with measured trajectories and a variety of contextual information to output the prediction in a local occupancy grid map in polar coordinates. By using polar coordinates, a reliable movement model is learned as base model being insensitive against blind spots in the data. The model is further improved by considering input features containing information about the static and dynamic environment as well as local movement statistics. The model successfully predicts multiple movement options represented in a polar grid map. Besides, the model can continuously improve the prediction accuracy without re-training by updating local movement statistics. Finally, the trained model is providing reliable predictions if applied on a different intersection without data from this intersection.

1 INTRODUCTION

The 2015 status report on road safety by the World Health Organization states that 1.25 million road traffic deaths occur every year (WHO, 2016b). 275.000 of those 1.25 million or 22 % are pedestrians and an additional 4 % are bicyclists. This is mainly due to the fact, that those two groups belong to the class of non-motorized road users, which are the most vulnerable class, the Vulnerable Road Users (VRUs). The WHO states that it is an important goal to make traffic participation for VRUs safer. (WHO, 2016a).

In general, pedestrians are advised to cross a street only at designated crosswalks or intersections with traffic lights. However, especially at intersections with multiple driving lanes or at unsignalized intersections, pedestrians must keep attention on the traffic. Using a mobile phone while crossing a street can lead to a severe lack of attention and fatal accidents (Hatfield and Murphy, 2007). Automated and assisted driving should help to prevent accidents between VRUs and vehicles. However, especially in urban scenarios, where scenes are cluttered by obstacles, trees and other cars, the onboard sensors are limited. In order to still be able to recognize pedestrians with high precision, cooperative perception systems could be used (Kim et al., 2013). Those systems use the fusion of sensor data from different sources to model a more precise surrounding of the car than by using the on-board sensors alone. For that, the car communicates not only with other cars but also with the infrastructure via Vehicle-to-Everything (V2X) communication (Rauch et al., 2012).

Sensors integrated into the infrastructure can provide an elevated view on crowded scenes and offer very precise sensor data about all traffic participants. This approach was investigated in research by e.g. the I2EASE project. Within the project, information from infrastructure sensors, vehicle sensors and VRU localization devices is sent to a central intersection computer to generate a fusion of all the incoming data, which then can be used for further applications such as the prediction of road user movement. (Bock et al., 2017). Another project inspecting the use of infrastructure mounted sensors and X2X-communication station is the research intersection built by DLR in Braunschweig, Germany (Schnieder et al., 2016). They installed four multi-

Bock, J., Nolte, P. and Eckstein, L.
Continuously Improving Model of Road User Movement Patterns using Recurrent Neural Networks at Intersections with Connected Sensors.
DOI: 10.5220/0007675603190326
In *Proceedings of the 5th International Conference on Vehicle Technology and Intelligent Transport Systems (VEHITS 2019)*, pages 319-326
ISBN: 978-989-758-374-2

sensor systems to measure road users at this intersection. Such data could be used in the context of cooperative driver assistance systems or complete autonomous driving features.

Sensors integrated into the infrastructure can not only help to prevent accidents but also to improve traffic flow, especially on crowded hot-spots like intersections (van Arem et al., 2006). Automated or assisted driving functions can prevent critical situations with pedestrians before they actually happen by predicting the movement of pedestrians. For this, data-driven machine learning approaches can be used.

2 RELATED WORK

In 2015, Goldhammer et al. (Goldhammer et al., 2014) developed a Neural Network (NN) to predict a pedestrians trajectory for the next 2.5 seconds. The approach of using a NN was used to compare its capabilities in contrast to the commonly used Kalman-filter method and approaches using only a NN without polynomial input. The data for training the NN was acquired by installing a camera at an intersection and filming uninstructed pedestrians in a natural environment and the used network was a multi-layer perceptron. The result was a significantly better prediction performance than with the Kalman-filter and also better performance than predicting the trajectory without the polynomial input .

Another approach of predicting pedestrians trajectories with NNs was presented in 2017 by Pfeiffer et al. (Pfeiffer et al., 2017). They integrated the surroundings of the pedestrians into the prediction to include static obstacles influencing the path. Another difference is, that they used a grid map to store not only information about static surroundings but also information about other pedestrians, which inundate the observed one. Used data were a combination of simulated data and the ETH dataset (Pellegrini et al., 2009). The prediction task was interpreted as a sequence modeling task, therefore a Long Short-Term Memory (LSTM) network was used. The complete network consists of a joint LSTM, which takes three inputs: The first input is the current velocity of the observed pedestrian, the second is a two-dimensional occupancy grid, which holds information about static obstacles in the area. The third input is a radial grid which is centered on the observed pedestrian and holds information about surrounding pedestrians. The result was a significantly lower prediction error for the LSTM approach compared to the baseline models.

Similar to this approach is the network architecture proposed by Varshneya et al. in 2017 (Varshneya and Srinivasaraghavan, 2017). They contended a Spatially Static Context Network (SSCN), which uses LSTM and also includes static environment information in the trajectory prediction. For training, they used the ETH dataset, the UCY dataset (Lerner et al., 2007) and the Stanford dataset (Robicquet et al., 2016). The proposed network uses three input streams. The first stream takes class labels as an input to indicate to which class the currently considered object belongs to. The second stream takes the current image of the considered object as well as pictures of the surroundings of the object. The third stream uses the whole image of the observed scene as a context. The evaluation showed, that the proposed SSCN outperformed the raw LSTM approach.

In 2016, Alahi et al. proposed a data-driven human-human interaction aware trajectory prediction approach (Alahi et al., 2016). They build a LSTM model, predicting the trajectories of pedestrians while also incorporating their interaction with each other, called Social-LSTM. The used datasets were the ETH dataset and the UCY dataset. Their network is a pooling-based LSTM model, which predicts the trajectories of all the people in the scene. In particular, there is one LSTM for each person in the scene. However, since one LSTM per person would not capture interactions between neighboring persons, adjacent LSTMs are connected by a pooling layer. With this, every LSTM cell receives a pooled hidden state of its neighbors. The network was compared to multiple other implementations, ranging from a linear Kalman-filter to a LSTM using only the coordinates of neighboring pedestrians as an input to the pooling layers instead of the whole set of features (O-LSTM). The result was, that the Social-LSTM outperformed all other approaches.

Once more using a context-aware model, Bartoli et al. introduced such a context-aware LSTM in 2017 (Bartoli et al., 2017). They based their network on the Social-LSTM model by Alahi et al. (Alahi et al., 2016), but extended it by not only including interactions between humans but also between humans and the static environment. For training, they used the UCY dataset and a second self-created dataset from a museum. For evaluation, the network is compared to a raw LSTM, and two LSTMs considering human-to-human interaction. Each of those networks was then extended by the context awareness. For both datasets, the context-aware extensions of the networks performed better than their unaware counterparts.

Hug et al. introduced an approach of predicting multiple possible trajectories at once (Hug et al., 2018). The reason behind this approach is to make a more robust risk assessment respectively a risk measurement capturing the uncertainty when predicting different options for action than predicting only the most probable one. For this a model combining a LSTM with a Mixture Density Layer (MDL) is introduced. The discrete position of the observed pedestrians serves as an input, while the output is a set of parameters for a Gaussian Mixture Model, which describes the offset from the current to the next position of the pedestrian. This generated Gaussian mixture model is combined with a particle filter. Qualitative evaluation was done by using two scenes from the Stanford Drone dataset and inspecting the results visually.

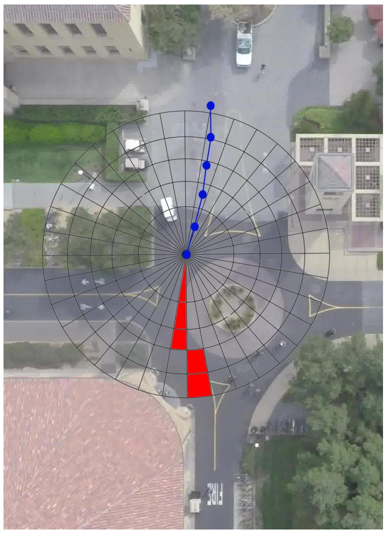

Figure 1: Example of a radial grid centered on the last observed position of a road user illustrated on image from the Stanford Dataset (Robicquet et al., 2016).

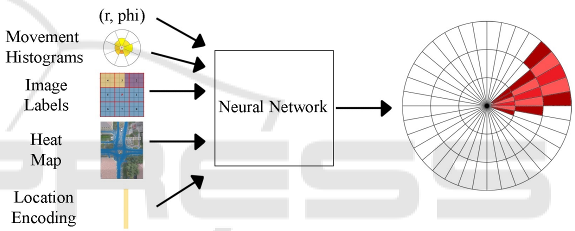

Figure 2: Input and Output Structure of the Network.

3 METHOD

Analyzing the state-of-the-art approaches leads to the need for a data-driven model capturing the uncertainty of its prediction while being able to learn continuously over time and considering the static and dynamic environment. Furthermore, the method need to be valid for several intersections and not just a single one. Based on this, we defined certain requirements for our model:

First of all, the model should put out a prediction capturing the uncertainty of its prediction, meaning that computing a most probable path for a given trajectory is not enough. This requirement is fulfilled by computing a local occupancy grid, centered on the last observed position of the traffic participant to predict.

In addition to that, the model should be transferable to other intersections after it is learned on several different intersections. Futhermore, it should be able to make reliable predictions for a trajectory from an area where no training data is present. For that, we propose not to use only plain x,y coordinates but rather location-independent coordinates as input and store the location-dependent information in the input features and not in the NN.

Furthermore, the model should consider the static and dynamic environment. I.e., considering static obstacles like buildings or barriers and also dynamic changes like the movement of other traffic participants. This is done by adding the contextual information as further input features.

As every intersection has its own characteristics and typical movement patterns, these shall be considered in the prediction. This information shall be contained in the input features. The NN shall learn to use contextual information in the input features and not learn the movement patterns directly. One of these contextual information would be a statistical distribution in which directions most people walk from a given position. By counting directional statistics over time, continuous learning is possible. Furthermore, a heat map indicating which areas in the environment are likely to be walked on by pedestrians is also used.

In order to be able to apply the prediction system without any data from this intersection, models should be transferable. This is done by learning a movement model of pedestrians at intersections in general from multiple dataset from arbitrary intersections.

Finally, the model should be able to continuously learn and improve its prediction capability. For that, we propose continuously improving by updating input features of e.g. the input features containing intersection specific patterns.

All those input features are then combined into one LSTM-based NN model (see Fig. 2). The grid map-based approach by Kim et al. and Park et al. is promising for a model capturing the uncertainty of its prediction since it is possible to represent options of action (Kim et al., 2017) (Park et al., 2018). Thus, a local grid map, centered on the observed pedestrian is the output of the network (see Fig. 1).

4 IMPLEMENTATION

Within this chapter, details about the implementation of the presented prediction model concept are given. Due to the use of a grid map as prediction output, an euclidean distance metric is not directly applicable and new metrics are needed. Thus, new metrics for evaluating grid maps are proposed in this chapter.

4.1 Data Preprocessing

The first step of data preprocessing is a resampling step to a sample rate of 2.5 Hz. After splitting the sequence in a training and a test set with a relation of 80:20, the sequences are enriched by additional input features. Then, the sequences are separated into input and output snippets, where an input length of 10 steps and an output length of six steps is chosen. This corresponds to four seconds of observation and a prediction horizon of 2.4 seconds. The input trajectories of the training and the test set are normalized sequence-wise to have a mean of zero and a variance of one.

4.2 Transferability

To ensure transferability of the model, the input sequences cannot be in Cartesian coordinates. If they were, the network would most likely overfit based on trajectories which it would see often. This would, for example, happen in a scene, where there is a very crowded entrance attracting many pedestrians. Transferring the model learned on this data to another intersection would result in predicting trajectories in the same area as if there were a similarly crowded area. Since this is something to prevent, the coordinates must not be absolute but rather relative ones, which is done by converting the input trajectory coordinates to relative polar coordinates.

4.3 Static Environment

Static map data is different for every intersection but does not contradict the requirement of transferability since static map information can easily be created for every intersection. For the static map, four different labels are applied to the scene, which results in the colored image in Fig. 3. Red encodes buildings and solids, Blue represents streets, Violet grass, bushes or trees and Yellow indicates sidewalks. The values of the different areas are used as input for the network in a nine-dimensional vector. This vector includes the label of the current position and the labels of the surroundings in eight directions. For every direction, the

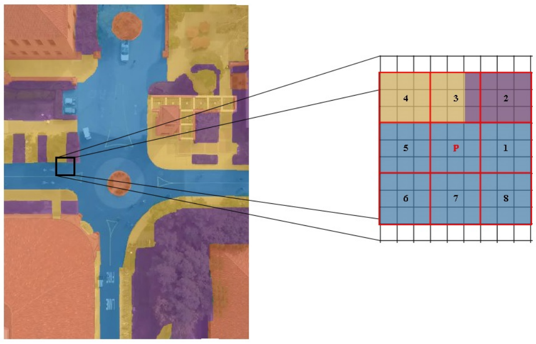

Figure 3: Retrieval of surrounding static map data(image labels).

mean label of the corresponding area is calculated, where the size of the area can be parameterized. I.e., if the label of direction 3 with an area size of 3 by 3 in Fig. 3 should be calculated, the center of the upper middle quadrant is chosen.

4.4 Dynamic Environment

Besides the static environment, the dynamic environment needs to be considered. As only pedestrians and bicyclists are contained in the used dataset, only these traffic participants are taken into account. As a simple representation, an occupancy grid-map containing how many people are around a given person at a particular time step is calculated. For every time step, a grid is initialized over the whole area of the scene, where the size of each grid cell can be parameterized and each cell is initialized with zero. Experiments showed, that the best performing grid cell size is 16 by 16 pixels. To fill the grid for every time step, the value in a cell in a grid for a particular time step is increased by one if and only if there is an observed traffic participant at this time step in this cell.

As a more sophisticated alternative to the simple occupancy grid map, another representation was built. Since the occupancy gridmap only captures how many other traffic participants are in a certain direction, basically three important pieces of information are missing: the distance, movement direction and velocity of those road users. Our proposed solution to this is the encoding of the surroundings using an autoencoder (Bengio et al., 2013). Similarly to the time step-indexed map used for the occupancy grid, the same matrix structure is created. However, instead of creating one matrix for every time step, only one matrix for every five time steps is used, which encodes the information of all time steps. This leads to one matrix representing the positions of every traffic participant currently on the scene during five time steps. This makes it possible to capture movements in

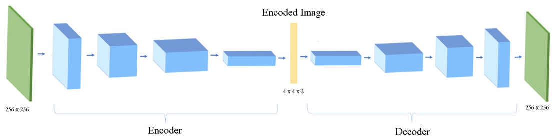

Figure 4: Autoencoder structure.

a small matrix. The resolution of the positions on the scene is scaled down by half. As structure of the autoencoder, a Convolutional Neural Network (CNN)-autoencoder is chosen, which reduces the input dimension of 256 by 256 to a representation of 4 by 4 by 2 and then back to 256 by 256. The structure of the autoencoder can be seen in Fig. 4.

During preprocessing the data, for every step in the trajectory, the current surroundings of the corresponding traffic participant are calculated. This image of the surroundings in the size of 256 by 256 pixels are then passed into the saved encoder. The result is a 32-dimensional representation of the surroundings, which includes the paths of every other road user in the area during the last five time steps.

4.5 Intersection-specific Patterns

There are two kinds of intersection-specific patterns, which are used in the model: Firstly, statistical histograms counting how many people are going to which direction from the current position. Secondly a heat map, which resembles at which positions at the intersection pedestrians are often present.

For the movement direction histograms, the possible directions are reduced to eight directions, i.e., every direction has a range of 45 degrees. The initial directional movement values are $\frac{1}{8}$, because the chance to go in the eight different directions from the current position is the same for every direction. The corresponding data structure contains a matrix with as many rows and columns as there are pixel in the scene image. Every cell represents a pixel P in the scene and contains an eight-dimensional vector V, where, for every direction $D1$ - $D8$, the number of traffic participants going into this direction on average from point P is saved. The size of the area which is recognized as one direction is parametrizable. Experiments showed that the best performing size is 16 by 16 pixels. This leads to a data structure, which holds a histogram over eight movement directions from any given point on the scene.

The heat map is built as a matrix in the size of the intersection scene in pixels. Every cell of this matrix represents a position a traffic participant can have in the scene. To fill this matrix, a counter starting at zero is increased whenever a person in the scene appeared at that cell. During the preprocessing, the position P of the currently observed traffic participant is calculated with regard to the chosen cell size of the heat map. Similarly to the occupancy grid map, the heat map values in eight directions from the position P are extracted from the datastructure.

Both input features support the requirement of continuous learning, because they can be improved over time by updating the statistics using the newly observed data.

4.6 Gridmap Output

Because the input trajectory is represented in polar coordinates, the grid maps used as output are radial polar coordinate grids. A resolution of five degrees is chosen for the angle, and a resolution of five to one is chosen for the radius.

Implementation-wise, the label is represented as a matrix. Every row represents an angle of five degrees, and every column represents a radius of four pixels, which results in a dimension of 72 by 80. The 80 columns come from approximating the maximum distance of a traffic participant during the prediction time to less or equal to 400 pixels. The conversion factor from pixels to meters is 0.037 for the used dataset, which equals in a maximum distance of 14.8 meters during 2.4 seconds. This corresponds to a speed of around 22 km/h, which we consider as sufficient for pedestrians.

4.7 Neural Network Model

The Neural Network model is implemented using Keras (Chollet et al., 2015). In the proposed model, Gated Recurrent Units (GRUs), a variant of Recurrent Neural Networks (RNNs) similar to LSTMs are used.

Our best performing model consists of two dense layers and three stacked GRUs layers. The input of the network represents a masking layer to allow short observations as input. After this masking layer there are three stacked GRU layers with 128 neurons each. *Tanh* is used as an activation function and a *hard sigmoid* is used as a recurrent activation function.

After the GRU layer, there are two fully connected layers with the first consisting of 16 neurons with a *relu* activation function. The second fully connected layer is the output layer of the network. It consists of 5760 neurons, which equals to the dimensions of the grid map labels. The *sigmoid* function is chosen as an activation function for this layer.

The model was trained using the Adam extension AMSGrad for 200 epochs. As error function the categorical crossentropy function is chosen.

4.8 Metrics

For evaluation, new metrics were necessary. Thus, we propose the metrics Mean Overlapping Percentage (MOP), Partwise Overlapping Percentage (POP), Mean Percentage (MP) and Wrong Percentage (WP) metric. The Combined Metric Value (CMV) combines all presented metrics in one rating value.

The Categorical Cross Entropy Error (CCE) metric is used to capture the difference between the correct label for one input trajectory and the output of the model.

$$-\Sigma x_{true} \times log(x_{pred}) \tag{1}$$

It is calculated as a sum of the discrepancy of all labels with their corresponding model outputs.

The Mean Overlapping Percentage (MOP) metric is used to capture how much of the true trajectories are completely overlapped by the output grid map on average. For every correct label (x_{true_i}) it is checked, if every position marked with a one in the label has a corresponding probability value in the model prediction (x_{pred_i}), which is higher than the threshold. If this is true for all positions in the label, the label is completely overlapped. If this is wrong for at least one of the positions, the complete label is not overlapped. This metric punishes a prediction which is incorrect but can be bypassed by always predicting a very high percentage for every grid map cell. Getting a high score in this metric should ensure, that all true trajectories are predicted but also, that multiple different movement options are predicted.

The Partwise Overlapping Percentage (POP) metric captures, how much of each true trajectory is overlapped by the model output on average. For every label, it is checked if the model output overlaps every point. If the corresponding position in the model output grid map has a probability value greater than a threshold, it is marked with a one, else it is marked with a zero. Then the average for each label separately is calculated and afterward the average over all averages. This metric also punishes wrong predictions but gives greater insights into how good the prediction actually is. Similarly to the MOP metric in can be bypassed by always predicting an occupancy probability of 100 % for every cell in the output.

The Mean Percentage (MP) metric calculates what the average chance of occupancy for the correct positions is. This metric ensures the exactness of the prediction by punishing the prediction of cells, which are near but not exactly the right ones. Once again it can be bypassed by always predicting the occupancy probability of all cells with 100%.

To counter the bypassing capabilities of the MOP, POP and MP metric, the Wrong Percentage (WP) metric is used. This metric captures the average difference of the true label and the prediction. Similarly to the Kalman filter predictions, the labels for this metric are enhanced by applying a 3 by 3 discrete Gaussian filter onto every cell marked with a one in the label. The metric then subtracts the correct probability value for every cell from the probability value the model predicted. This is done for every label and is averaged afterward. This metric heavily punishes wrong predicted cells and is a counterweight to the last three metrics. Since it also not wanted, that only the, for the model, single correct trajectory is predicted but instead also different movement options at the same time, this cannot be the only metric but it has to be combined with all the other metrics.

This is done by the last metric, the Combined Metric Value (CMV). This metric combines all presented metric in one rating value. The higher the value is, the better the prediction behaves while computing predictions of different movement options but also not assigning too high occupancy probabilities to all the cells in the grid map.

$$\frac{(MOP + POP + MP)}{\left(\frac{CCE}{100} + WP \times 10\right)} \tag{2}$$

The value for the CCE metric is scaled down since it can range between zero and ∞, while the value for the WP metric is scaled up since it normally ranges between 0 and 0.005. Furthermore, its influence to rating the model is crucial as a counterweight to the MOP, POP and MP metrics. In addition to that, the MOP, POP, and MP metrics are calculated stepwise. I.e., those metrics are not only calculated for every complete trajectory but also separately for every first step of the trajectory, the first two steps of it and so on. This captures the decreasing capabilities of the model for predictions over a longer prediction horizon.

5 RESULTS

For evaluation, a traditional linear Kalman filter is used, which is a common practice in literature. As dataset the DeathCircle scene of the Stanford Drone dataset is used (Robicquet et al., 2016).

The proposed model was amongst other things evaluated with regard to additional information improving the prediction capabilities. To evaluate this, seven different stages of additional input features were compared:

1. Only relative polar coordinates
2. As in 1. plus static map data

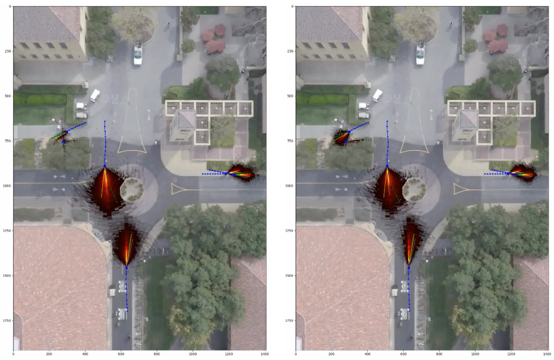

(a) Model with naive grid (b) Model with encoding
Figure 5: Comparison of the Model Prediction.

3. As in 2. plus histograms
4. As in 3. plus naive occupancy grid
5. As in 4. plus heat map
6. As in 5. plus x,y coordinates
7. As in 5. but with encoded surroundings instead of naive occupancy grid

The first evaluated model reaches a CMV value of 10.879. Especially the CCE value is with 11.056 relatively high, while the WP error is with 0.00227 extremely low. However, already adding the static map data as additional input features improves the CMV value to 11.330. The CCE value is lowered to 9.482, but also the WP increases to 0.00477. However, all of those first six models are inferior to the model using all the additional input features but replacing the naive occupancy grid approach with the encoded local surroundings and the basic x,y coordinates. This results in a CMV of 11.790 with a CCE value of 9.450 and a WP value of 0.00434, where all those values are highly significantly better than their prior counterparts. This is also achieved when evaluating the already trained network with smaller fractions of the sequences with regard to the histograms and the heat map. Especially the CMV decreases from 11.790 to 8.248 while only using 10 % of the sequences.

In Fig. 5 two different models are compared qualitatively. In each picture, the blue dotted line represents the observed trajectory, the green one denotes the true future trajectory, the yellow line indicates the prediction of the Kalman filter, and the heat map in red describes the model output. The prediction for the trajectory entering the roundabout from above contains more possible movement options for the right than for the left model. This is for this specific area a valid result since it is possible that, even while approaching the roundabout in a very straightforward manner, the traffic participant will turn and leave the roundabout in westward direction. This is also a difference for the road user arriving at the roundabout from underneath. The prediction depicted on the left already predicts a possible left or right turn, but the roundabout is yet relatively far away. The prediction of the right model makes for this position a lot more sense.

Furthermore, the model using the naive grid tends to learn a cross-shaped prediction for traffic participants not moving. This can be seen on the right for the pedestrian at position (250, 750) next to the arriving pedestrian. This form of prediction does not happen for the model using the Encoding. The predictions of the two pedestrians on the right side of the image and the walking pedestrian at position (250, 700) are equally good in both models.

6 CONCLUSIONS

In this paper, we presented a new approach to predict trajectories, which at the same time captures the uncertainty in prediction by a polar grid map, is transferable to other intersections, considers static and dynamic environment information as well as scene-specific patterns and is able to improve continuously over time with new measurement data without retraining the model.

The proposed model was evaluated via different metrics and compared for different sets of input features and also with the basic Kalman filter prediction approach. This evaluation resulted in a significantly better prediction when using the proposed set of input features, containing relative polar coordinates, static map data, movement histograms, a movement heat map, an encoding of the surrounding traffic participants and the plain Cartesian coordinates. Our results show significantly better scores for all introduced metrics compared to the Kalman filter, which is supported by qualitative evaluations.

We plan to enhance the proposed model in the future by an improved encoding of the dynamic environment. Furthermore, we plan to create a statistical baseline model for predictions with grid maps as output based on measurement data from intersections.

ACKNOWLEDGEMENTS

The work for this paper was partially funded within the project I2EASE funded by the German Federal Ministry of Education and Research based on a decision of the German Federal Diet.

REFERENCES

Alahi, A., Goel, K., Ramanathan, V., Robicquet, A., Fei-Fei, L., and Savarese, S. (2016). Social LSTM: Human trajectory prediction in crowded spaces. In *2016 IEEE Conference on Computer Vision and Pattern Recognition (CVPR)*. IEEE.

Bartoli, F., Lisanti, G., Ballan, L., and Del Bimbo, A. (2017). Context-aware trajectory prediction. *arXiv preprint arXiv:1705.02503*.

Bengio, Y., Courville, A., and Vincent, P. (2013). Representation learning: A review and new perspectives. *IEEE Transactions on Pattern Analysis and Machine Intelligence*, 35(8):1798–1828.

Bock, J., Beemelmanns, T., Klösges, M., and Kotte, J. (2017). Self-learning trajectory prediction with recurrent neural networks at intelligent intersections. In *Proceedings of the 3rd International Conference on Vehicle Technology and Intelligent Transport Systems*.

Chollet, F. et al. (2015). Keras. `https://github.com/fchollet/keras`.

Goldhammer, M., Doll, K., Brunsmann, U., Gensler, A., and Sick, B. (2014). Pedestrian's trajectory forecast in public traffic with artificial neural networks. In *2014 22nd International Conference on Pattern Recognition*. IEEE.

Hatfield, J. and Murphy, S. (2007). The effects of mobile phone use on pedestrian crossing behaviour at signalised and unsignalised intersections. *Accident Analysis & Prevention*, 39(1):197–205.

Hug, R., Becker, S., Hübner, W., and Arens, M. (2018). Particle-based pedestrian path prediction using lstm-mdl models.

Kim, B., Kang, C. M., Lee, S., Chae, H., Kim, J., Chung, C. C., and Choi, J. W. (2017). Probabilistic vehicle trajectory prediction over occupancy grid map via recurrent neural network. *CoRR*, abs/1704.07049.

Kim, S.-W., Chong, Z. J., Qin, B., Shen, X., Cheng, Z., Liu, W., and Ang, M. H. (2013). Cooperative perception for autonomous vehicle control on the road: Motivation and experimental results. In *2013 IEEE/RSJ International Conference on Intelligent Robots and Systems*. IEEE.

Lerner, A., Chrysanthou, Y., and Lischinski, D. (2007). Crowds by example. In *Computer Graphics Forum*, volume 26, pages 655–664. Wiley Online Library.

Park, S., Kim, B., Kang, C. M., Chung, C. C., and Choi, J. W. (2018). Sequence-to-sequence prediction of vehicle trajectory via lstm encoder-decoder architecture. *arXiv preprint arXiv:1802.06338*.

Pellegrini, S., Ess, A., Schindler, K., and van Gool, L. (2009). You ll never walk alone: Modeling social behavior for multi-target tracking. In *2009 IEEE 12th International Conference on Computer Vision*. IEEE.

Pfeiffer, M., Paolo, G., Sommer, H., Nieto, J. I., Siegwart, R., and Cadena, C. (2017). A data-driven model for interaction-aware pedestrian motion prediction in object cluttered environments. *CoRR*, abs/1709.08528.

Rauch, A., Klanner, F., Rasshofer, R., and Dietmayer, K. (2012). Car2x-based perception in a high-level fusion architecture for cooperative perception systems. In *2012 IEEE Intelligent Vehicles Symposium*. IEEE.

Robicquet, A., Sadeghian, A., Alahi, A., and Savarese, S. (2016). Learning social etiquette: Human trajectory understanding in crowded scenes. In *European conference on computer vision*, pages 549–565. Springer.

Schnieder, L., Knake-Langhorst, S., and Gimm, K. (2016). AIM research intersection: Instrument for traffic detection and behavior assessment for a complex urban intersection. *Journal of large-scale research facilities JLSRF*, 2.

van Arem, B., van Driel, C. J. G., and Visser, R. (2006). The impact of cooperative adaptive cruise control on traffic-flow characteristics. *IEEE Transactions on Intelligent Transportation Systems*, 7(4):429–436.

Varshneya, D. and Srinivasaraghavan, G. (2017). Human trajectory prediction using spatially aware deep attention models. *arXiv preprint arXiv:1705.09436*.

WHO (2016a). Developing global targets for road safety risk factors and service delivery mechanisms. `http://www.who.int/violence_injury_prevention/road_traffic/road-safety-targets/en/` [accessed in February 2019].

WHO (2016b). Global status report on road safety 2015. `http://www.who.int/violence_injury_prevention/road_safety_status/2015/en/` [accessed in February 2019].